

# An Empirical Propagation Model for Mobile Radio Links in Container Terminal Environment

Slawomir J. Ambroziak and Ryszard J. Katulski, *Member, IEEE*

**Abstract**—In the article a novel empirical propagation model for mobile radio links in a container terminal environment is presented. Measurement propagation research carried out in Gdansk Deepwater Container Terminal in Poland is described and the investigated environment is characterized. The results of statistical evaluation of the new model are discussed. In addition, a statistical tuning of the Walfisch-Ikegami model for the investigated environment is presented.

**Index Terms**—path loss modelling; propagation losses; radiowave propagation;

## I. INTRODUCTION

The container port area should be treated as a very difficult radio wave propagation environment, because the large number of steel containers cause a very strong multipath effect and there is a time-varying container arrangement in stacks of different height. Path loss modelling for such an area remains a complex task that is not considered enough in scientific research. So far a number of propagation models have been developed, but mainly for urban and rural areas [1]-[5] and it should be noted that ITU-R did not present any special recommendation for path loss (so-called basic transmission loss [6]) prediction of radio link in the container terminal environment. It is commonly known that other models for urban or suburban areas are used for this purpose, but differences in spatial arrangement and structure between container stacks and buildings in a typical urban area may cause substantial path loss prediction errors when applying an unsuitable propagation model. Therefore, a special survey of the propagation phenomena in the container terminal area becomes crucial. Admittedly, there is a propagation model aimed at the container port environment, but this model was developed for designing only fixed radio links and does not take into account many factors occurring in the environment under investigation [7], [8]. Modelling basic transmission loss in mobile radio links is more complicated, so it is particularly important to elaborate a new propagation model that could be useful for designing such links. It should be noted that there are no similar comprehensive works for mobile radio links working in the environment that is considered in this article.

In [9] and [10] the selected propagation models were

evaluated in terms of designing mobile radio networks in the environment under investigation. These models were also adjusted by adding correction functions, which was described in [11] and [12]. The evaluation as well as the adjustment underlined the necessity of elaborating of a new path loss model for this environment.

This article describes a novel empirical propagation model for mobile radio links in the container terminal environment. At the outset of the article, in section II, the measurement equipment as well as the measurement procedures used for propagation research in Deepwater Container Terminal in Gdansk, Poland (hereinafter called DCT Gdansk) are described. Next, in section III, the investigated environment is characterized. In the main part of the article (section IV) a new approach to path loss modelling in the case of radio wave propagation in the container port, based on empirical results from measurement campaigns in DCT Gdansk, is presented. This novel empirical model was elaborated on the basis of almost 290 thousand propagation path measurements in real conditions. This model has been named MCT, as an abbreviation for: mobile, container, terminal. Afterwards, in section V, the results of statistical evaluation of the new model are presented. At the end of the article (section VI), a statistical tuning of the Walfisch-Ikegami model for the investigated environment is presented. This modified model is also compared with its original form.

## II. MEASUREMENT EQUIPMENT AND PROCEDURES

The measurement equipment which was used during research in DCT Gdansk consists of a fixed transmitting section and a mobile receiving section. It was developed for carrying out semi-automated propagation measurements in accordance with the normative requirements described later in this section.

A block diagram of the fixed transmitting section is presented in Fig. 1. The signal generator (Agilent E4433B) is the source of the BPSK test signal with a bit rate of 3 kbps. For frequencies from 800 MHz to 4.2 GHz an RF amplifier (Amplifier Research 5S1G4) is used.

Slawomir J. Ambroziak is with the Department of Radio Communication Systems and Networks, Faculty of Electronics, Telecommunications and Informatics of Gdansk University of Technology, 11/12 Narutowicza Street, 80-233 Gdansk, Poland (e-mail: [sj\\_ambroziak@eti.pg.gda.pl](mailto:sj_ambroziak@eti.pg.gda.pl)).

Ryszard J. Katulski is with the Department of Radio Communication Systems and Networks, Faculty of Electronics, Telecommunications and Informatics of Gdansk University of Technology, 11/12 Narutowicza Street, 80-233 Gdansk, Poland (e-mail: [rjkat@eti.pg.gda.pl](mailto:rjkat@eti.pg.gda.pl)).

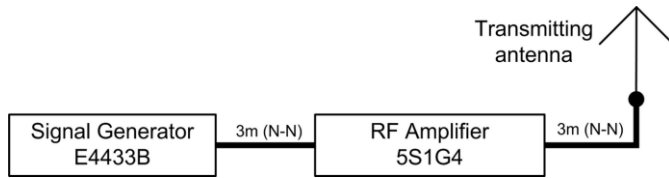


Fig. 1. Block diagram of fixed transmitting section.

For lower frequencies the signal generator is connected directly to the transmitting antenna, which is a monopole vertical antenna with an electrical length of one-quarter of a wavelength. It was developed and implemented in a manner that allows its linear length to be changed, so it may be used for research in various frequencies. The parameters of this antenna (for measured frequencies) are presented in Table I.

TABLE I

PARAMETERS OF TRANSMITTING/RECEIVING MEASUREMENT ANTENNA

Frequency [MHz]	Length [cm]	SWR	Gain [dBi]
500	15	1.86	2.3
1000	7.5	1.05	
2000	3.7	1.05	
4000	1.8	1.5	

The block diagram of the mobile receiving section, situated on the test vehicle, is presented in Fig. 2.

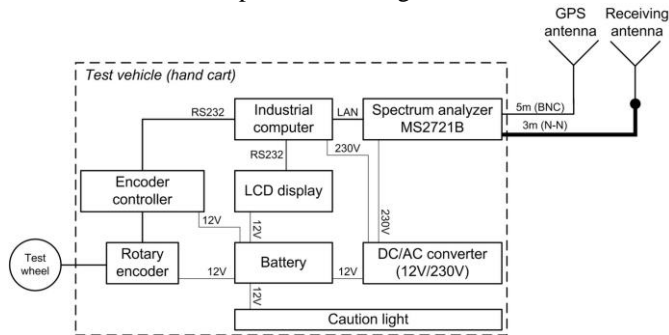


Fig. 2. Block diagram of mobile receiving section.

The receiving antenna is of the same type as the transmitting antenna and it is installed at a constant height of 2 m. As a measurement receiver, a spectrum analyser (Anritsu MS2721B) is used. It allows measurements in the frequency range of 9 kHz to 7.1 GHz. The analyser is equipped with a built-in GPS receiver for matching each measurement result with the measured positions. The use of a spectrum analyser for automated measurements as well as its operational parameters are in accordance with the requirements described in [13]. An industrial computer (AAEON TF-AEC-6911-A1) with appropriate software is used to control the work of the spectrum analyser (via Ethernet) and for collecting measurement data. This computer is also responsible for triggering sequential measurements based on control signals coming (via RS232) from a rotary encoder. Additionally, it sends data to the LCD display, showing the current values of the measured parameters and the status of the system. The rotary encoder with its controller and the test wheel are responsible for indicating points of measurement triggering and for converting test wheel rotation to the distance covered by the test vehicle. A caution

light ensures good visibility of the research team during measurements in the container terminal area. The whole receiving section is carried by the test vehicle (hand cart), but the speed  $V$  [km/h] of the receiver is limited. The speed depends on the frequency  $f$  [MHz] of the test signal and the minimum time  $t_r$  [s] given by the receiver specification to revisit a single frequency. It is expressed by the following equation [13]:

$$V_{[km/h]} \leq \frac{864}{f_{[MHz]} \cdot t_{r[s]}} \quad (1)$$

Since the measurement data should include information about slow and fast changes of the power flux density of the electromagnetic field (slow and fast fading, respectively), it is recommended to choose the points of measurement in an appropriate manner. These points were spaced every  $0.8 \lambda$  along a route of radio wave propagation and the results were averaged every  $40 \lambda$  [13], [14]. Such spacing of measurement points, along with the averaging interval, allows us to obtain for each point the averaged path loss value calculated from a subset of 50 uncorrelated samples. The required minimum number of samples is 36 [15]. These requirements were fulfilled during the research.

The method described above is the well-known Lee method and it is recommended by ITU-R in [13] and described in detail in [14]. This method allows us to obtain a 1 dB confidence interval around the real mean value.

The transmitting section (Base Station – BS) was installed on the ship-to-shore gantry crane (Fig. 3) at various heights above the ground.

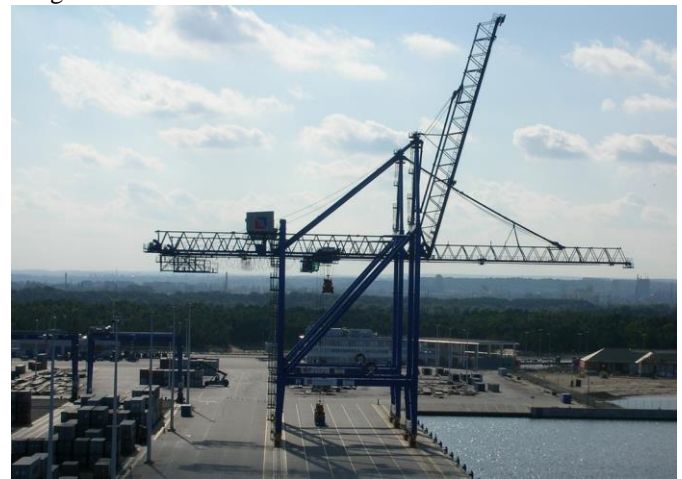


Fig. 3. The ship-to-shore gantry crane – the place of transmitting antenna installation.

Since the container terminal was in operation while measurements were being taken, the location of the gantry crane was variable along the quay and the line of BS movement is shown in Fig. 4 by the thick line.

The receiver (Mobile Station – MS) moved along the routes between the main container fields as shown in Fig. 4 by the thin line. It should be noted that during regular work of the container terminal there is heavy traffic of the container trucks in the area. This could be potentially dangerous for the research team. Due to this fact, the measurement path was chosen in such a way as to fulfill the safety regulations imposed by authorities at DCT

Gdansk.

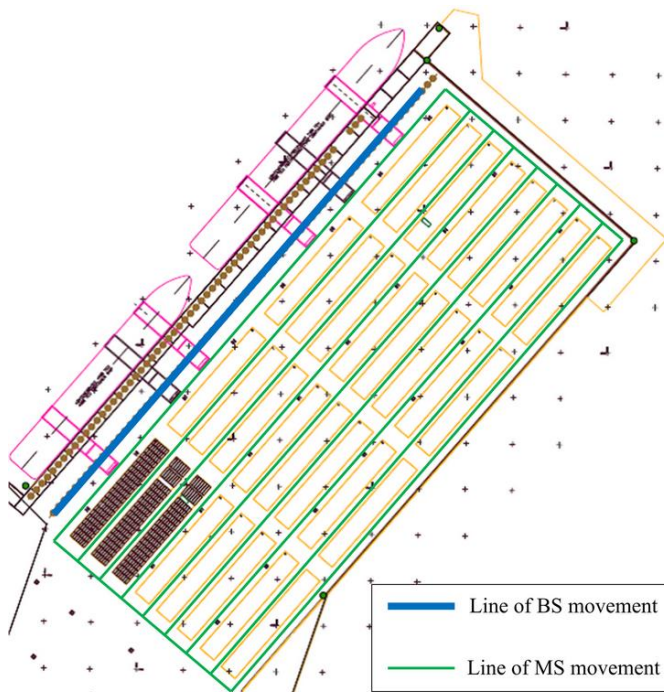


Fig. 4. The layout of DCT with marked movement lines of BS and MS.

During research in DCT, which was carried out in the years 2008 and 2009 in different seasons, nearly 290 000 measurement results were collected. It should be noted that for the analysed frequency range (less or equal 4 GHz) and distances (less than 620 m) the attenuation in rain, fog and atmospheric gases has no significant influence on the propagation path loss, what is described in details in [16], [17] and [18]. These measurement data formed the basis for the elaboration of the novel empirical model in the investigated environment with measurements performed at various propagation routes with different lengths (from a range of 50 m to 620 m), test signal at various frequencies (500 MHz, 1 GHz, 2 GHz and 4 GHz) and transmitting antenna of different heights (12 m, 24 m and 36 m). The receiving antenna height ( $h_{MS}$ ) was constant and equaled 2 m. It should be noted that measurements were taken for all four frequencies for each height of the transmitting antenna.

### III. INVESTIGATED ENVIRONMENT

Measurements were taken in the area of DCT Gdansk, which is built on an artificial peninsula surrounded by the Gulf of Gdansk on three sides. A view of DCT is presented in Fig. 5.



Fig. 5. View of the Deepwater Container Terminal in Gdansk, Poland.

Fig. 4 shows the layout of DCT with fields where the shipping containers are stored. A standard twenty-foot container is about 6.1 m long, 2.5 m wide and 2.6 m high. For a forty-foot container the length is about 12.2 m, but only

twenty-foot containers were taken into account and each forty-foot container was considered as two smaller twenty-foot containers. Their deployment is typical for this type of industrial environment and has a significant influence on radio wave propagation conditions. The area where the containers are stored is about twenty hectares. The length of this area is about 650 m and its width is about 310 m. Containers are stored on so-called main container fields, whose dimensions are 139.1 m long and 19.9 m wide. The main routes between these fields are 10 m wide and the perpendicular routes are 19.15 m wide.

The terminal consists of 32 main container fields, spaced in 8 rows, 4 fields for each row. Almost 154 stacks of the twenty-foot containers may be stored on each field, so the maximum number of all stacks does not exceed 4 928. At most, 5 containers may be in one stack, so the minimum height of a stack is 2.6 m and the maximum height of each stack does not exceed 13 m. It should be noted that the heights of container stacks are variable in time and could change significantly during one day. Therefore, up to 24 640 twenty-foot containers may be stored in the terminal area. Thus, the environment under investigation has a relatively regular structure, but the variability of heights of container stacks and their arrangement have a significant influence on the variation of the multipath. The statistical influence of this phenomenon is expressed by the characteristic variables of the model, which are described below. The diversity of conditions occurring in different places of the container terminal should also be taken into account in the new model. For this reason, the terminal was divided into three sub-areas, where different propagation mechanisms have a crucial influence on basic transmission loss (Fig. 6).

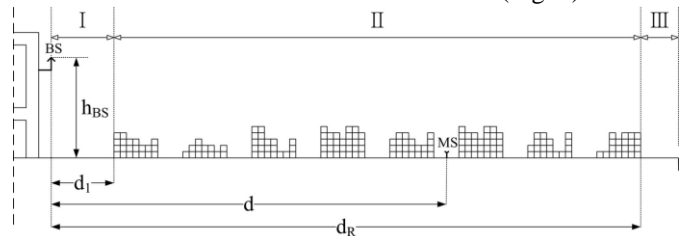


Fig. 6. Cross-section of the investigated terminal.

The first sub-area (I or the LOS Area) is defined for propagation path lengths ( $d$ ) shorter than the distance ( $d_1$ ) between the base station (BS) antenna and the first row of storage fields ( $d \leq d_1$ ). In this case, direct wave and waves reflected from containers in the first row, or reflected from the ground, have the predominant influence on radio signal power received by the mobile station (MS). This is shown in Fig. 7 by rays marked as 1. In this sub-area, the basic transmission loss depends on obvious factors such as frequency, path length, base station antenna height and the additional factor affecting the path loss: the average height of container stack ( $h_{c,1}$ ) in the first row.

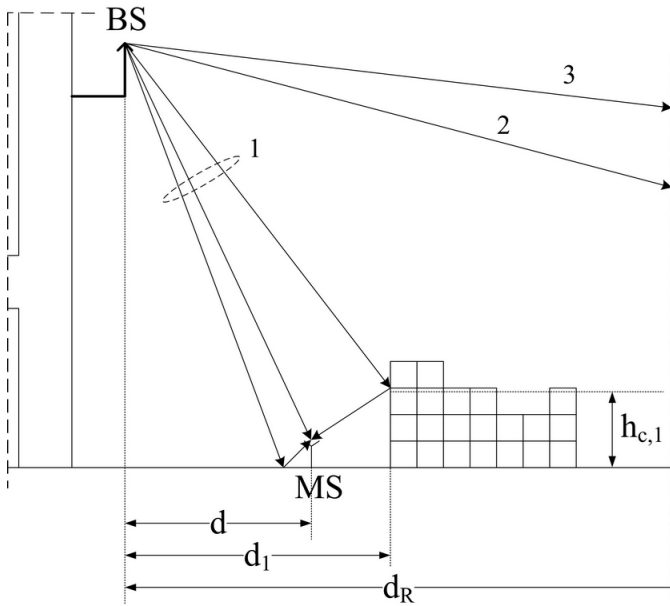


Fig. 7. An example scenario of radio wave propagation in the LOS Area.

The second sub-area (II or the Containers Area) is defined for propagation path lengths longer than  $d_1$  and shorter than distance ( $d_R$ ) between the base station antenna and the end of the last,  $R$ th, row of storage fields ( $d_1 < d \leq d_R$ ). In this case, the following phenomena have a predominant influence on the power of the received radio signal: diffraction at the edges of containers on the propagation path over the containers, especially at the edges of containers in the last,  $r$ th row of storage fields before the mobile station, and the wave reflection from the containers in the next row behind the mobile station. This is shown in Fig. 8 by rays marked as 2.

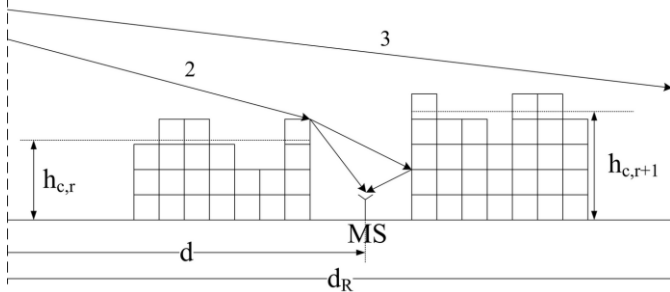


Fig. 8. An example scenario of radio wave propagation in the Containers Area.

Additional factors – except the obvious ones – affecting path loss in this sub-area are: average height of container stacks on the propagation path and average height of container stacks in the row behind the mobile station.

The third sub-area (III or the Off-Terminal Area) is defined for propagation path lengths longer than  $d_R$  ( $d > d_R$ ), where the diffraction at the edges of containers has a predominant influence on the received signal power. The mobile station receives just a small part of radio wave power due to diffraction at the edges of containers stored on fields in the last row. This is shown in Fig. 9 by rays marked as 3. Additional factors – except the obvious ones – affecting path loss, are as follows: average height of container stacks ( $h_{c,i}$ ) throughout the terminal and degree of surface occupancy of container stacks over the

entire surface of the terminal, expressed by the terminal surface occupancy ratio, defined below.

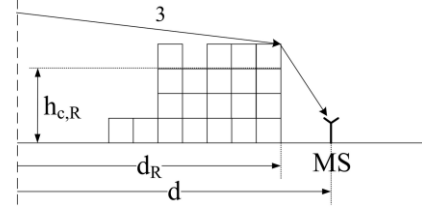


Fig. 9. An example scenario of radio wave propagation in the Off-Terminal Area.

Based on preliminary analysis of propagation conditions, the relevant factors affecting the basic transmission loss value in a container terminal environment were defined, namely:

- frequency ( $f$ ) of the radio signal,
- propagation path length ( $d$ ), defined as the distance (in the plane) between the base station antenna and the mobile station,
- base station antenna height ( $h_{BS}$ ),
- angle ( $\varphi$ ) of radio wave arrival between the direction of radio wave and the axis of the main routes between the storage fields (see Fig. 10).

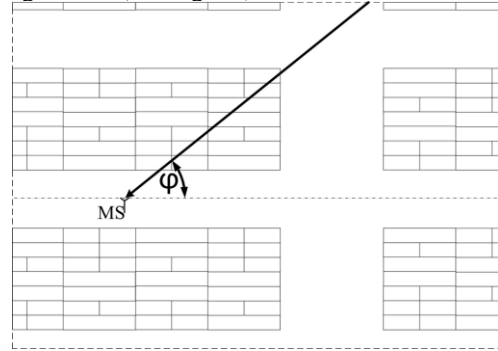


Fig. 10. Illustration of angle of radio wave arrival to the mobile station antenna.

The characteristic parameters for the investigated industrial environment are also very important. These are:

- terminal surface occupancy ratio ( $S_t$ ), defined as the ratio of surface occupied by containers to the whole terminal surface destined for container storage,
- $i$ th row surface occupancy ratio ( $S_i$ ), defined as the ratio of surface occupied by containers in the  $i$ th row to the whole surface destined for container storage in this row,
- average height of container stacks ( $h_{c,i}$ ) throughout the terminal,
- average height of container stacks ( $h_{c,i}$ ) in  $i$ th row,
- average height of container stacks ( $h_{c,d}$ ) over the propagation path length,
- average height of container stacks ( $h_{c,r+1}$ ) in the row behind the mobile station and causing the reflection of radio waves (see Fig. 8).

#### IV. THE NOVEL EMPIRICAL MCT MODEL

On the basis of the analysis of propagation conditions in each sub-area of the terminal under investigation, the basic transmission loss ( $L_{MCT}$ ) in such an environment may be expressed by the following equation:



$$L_{MCT[dB]} = \begin{cases} L_{LOS[dB]}, & \text{for } d \leq d_1, \\ L_{Com[dB]}, & \text{for } d_1 < d \leq d_R, \\ L_{OffT[dB]}, & \text{for } d > d_R. \end{cases} \quad (2)$$

Where the particular components are:

- for the LOS Area:

$$L_{LOS[dB]} = L_{0[dB]} - 4.2 \log(h_{BS[m]} - h_{c,l[m]}) + 11.6, \quad (3)$$

where the  $L_0$  factor is related to the direct wave, expressed by the well-known equation:

$$L_{0[dB]} = 20 \log f_{[MHz]} + 20 \log d_{[m]} - 27.6, \quad (4)$$

and the  $(h_{BS} - h_{c,l})$  factor is related to the wave reflected from containers in the first row of storage fields;

- for the Containers Area:

$$L_{Com[dB]} = 20 \log f_{[MHz]} + 25 \log d_{[m]} - 18 \log(h_{BS[m]} - h_{c,d[m]}) + 6.2 \log(h_{BS[m]} - h_{c,r+l[m]}) + 4 \log \varphi_{[^\circ]} - 21.8, \quad (5)$$

where the  $(h_{BS} - h_{c,d})$  factor is related to the path loss due to diffraction at the edges of containers on the propagation path over the containers, where:

$$h_{c,d} = \frac{\sum_{i=1}^r h_{c,i} \cdot S_i}{\sum_{i=1}^r S_i} \quad (6)$$

and the  $(h_{BS} - h_{c,r+l})$  factor is related to the wave reflected from the containers in the next row behind the mobile station;

- for the Off-Terminal Area:

$$L_{OffT[dB]} = 20 \log f_{[MHz]} + 30 \log d_{[m]} - 18 \log(h_{BS[m]} - h_{c,l[m]}) + 13.5 \log S_r + 4 \log \varphi_{[^\circ]} - 21.8, \quad (7)$$

where the  $(h_{BS} - h_{c,l})$  factor is related to the path loss due to diffraction at the edges of containers on the propagation path over the containers, where:

$$h_{c,l} = \frac{\sum_{i=1}^R h_{c,i} \cdot S_i}{\sum_{i=1}^R S_i} \quad (8)$$

and the  $S_r$  factor reflects the influence of the number of container stacks in the whole container terminal area. This factor is higher than 0 and lower than 1. It equals 1 when the whole terminal surface destined for container storage is occupied by the container stacks.

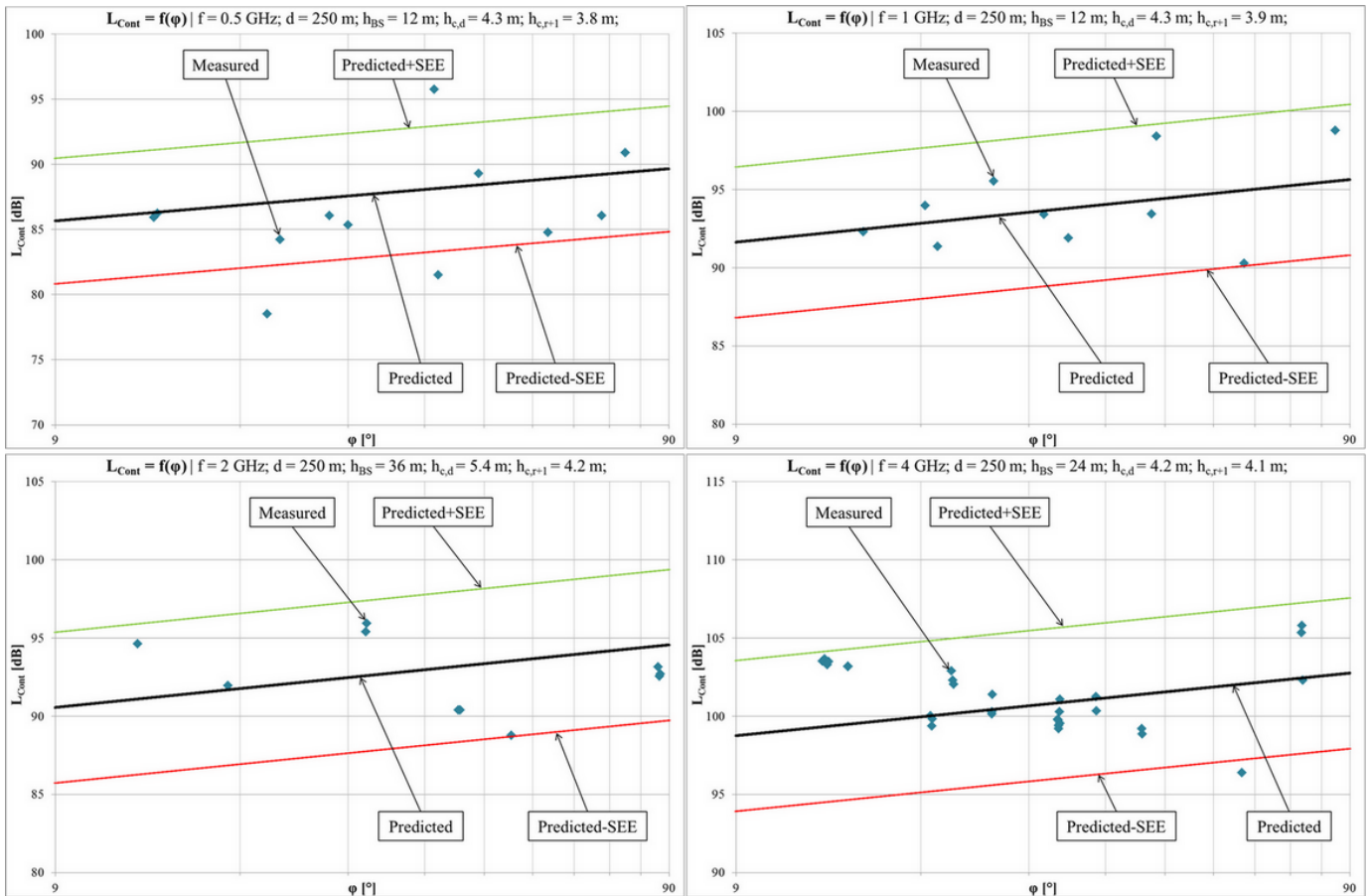


Fig. 11. Example graphs of path loss changes with respect to the angle of radio wave arrival for the Containers Area and for various frequencies.

In the above equations  $r=1,2,\dots,R-1$  is the number of the last row of storage fields before the mobile station and  $R$  is the number of all rows of storage fields. It should also be noted that the influence of the angle of radio wave arrival on the path loss is consistent with the experimental observation for urban areas, as described in [19], namely the path loss is low when the incident wave direction is nearly parallel to a street. This behaviour is observed at all measured frequencies, i.e. at 500 MHz, 1 GHz, 2 GHz and 4 GHz. This relation is shown in Fig. 11., where the example graphs of path loss changes with respect to the angle of radio wave arrival for the Containers Area and for various frequencies are presented. For each frequency, the measured values seem to correspond closely to the regression lines and in most cases they are in  $\pm$ SEE interval.

The  $i$ th row surface occupancy ratio ( $S_i$ ) and the terminal surface occupancy ratio ( $S_t$ ), reflect the number of containers stored in the  $i$ th row of main storage fields and on the whole terminal area, respectively. Considering equations (5)-(8), it may be said, that if the number of stored containers increases, the relevant surface occupancy ratio also increases, and the estimated path loss value increases too.

Coefficients of the MCT model equations were calculated on the basis of empirical data and using multivariate linear regression with the least-squares method, which minimizes the sum of squared differences between measured path loss value and the regression function. The statistical significance of particular coefficients was proven with a 95% confidence interval (5% level of significance) using the t-test with Student's distribution, and the statistical significance of regression functions was proven with the same confidence interval using the F-test with Fisher-Snedecor distribution.

The MCT model is valid for the following ranges of parameters:

- $500 \text{ MHz} \leq f \leq 4 \text{ GHz}$ ,
- $50 \text{ m} \leq d \leq 620 \text{ m}$ ,
- $12 \text{ m} \leq h_{BS} \leq 36 \text{ m}$ ,

and on the assumption that:

- $h_{BS} > h_{c,1}$ ,  $h_{BS} > h_{c,d}$ ,  $h_{BS} > h_{c,r+1}$  and  $h_{BS} > h_{c,t}$ ,
- $0 < \varphi \leq 90^\circ$ ,
- $0 < S_i \leq 1$ .

## V. STATISTICAL EVALUATION OF THE NEW MODEL

The statistical evaluation of the new MCT model is based on mean error (ME) and standard error of estimate (SEE). These errors are commonly used to verify the accuracy of the path loss models [5], [20], [21] and they are defined by (9) and (10) respectively [21], [22]:

$$ME_{[dB]} = \frac{1}{N} \sum_{i=1}^N (L_{m,i[dB]} - L_{c,i[dB]}), \quad (9)$$

$$SEE_{[dB]} = \sqrt{\frac{1}{N-1} \sum_{i=1}^N (L_{m,i[dB]} - L_{c,i[dB]})^2}, \quad (10)$$

where  $L_{m,i}$  is the measured value of the basic transmission loss in  $i$ th position of the receiver ( $i=1,\dots,N$ ),  $L_{c,i}$  is the basic transmission loss value computed using the propagation model

for the  $i$ th position, and  $N$  is the sample size. The mean error value reflects the expected average difference between path loss values obtained using the proposed model and real path loss measurements, while the standard error of estimate is the ratio of the dispersion of measured path loss values, and describes how well the propagation model matches experimental data.

Apart from these two parameters, a coefficient of determination ( $R^2$ ) is also very important. This is a statistical measure which tells what part of the path loss variability is explained by the independent variables used in the model. The coefficient of determination is calculated as a ratio of the regression sum of squares to the total sum of squares, which may be expressed by the following equation [23]:

$$R^2 = \frac{\sum_{i=1}^N (L_{c,i} - L_{m,av})^2}{\sum_{i=1}^N (L_{m,i} - L_{m,av})^2}, \quad (11)$$

where  $L_{m,av}$  is the averaged value of measured path loss and other parameters are as in (9) and (10).

Additionally, during the elaboration of the MCT model, one more statistic was used as well, namely the correlation coefficient ( $R$ ), which is a measure of linear dependence between path loss values calculated using a mathematical model and real measured values. Assuming that we do not consider the sign of this coefficient, it is calculated as the square root of the coefficient of determination [23]. Statistical evaluation for each sub-area of the investigated environment and for the entire MCT propagation model is summarized in Table II, where  $N$  is the number of collected measurements (sample size).

TABLE II  
STATISTICAL EVALUATION OF THE MCT PROPAGATION MODEL

Parameter	$L_{LOS}$	$L_{Cont}$	$L_{OffT}$	$L_{MCT}$
$N$	54 283	196 239	29 195	279 717
$ME$ [dB]	0.0	0.0	0.0	0.0
$SEE$ [dB]	4.56	4.82	4.25	4.71
$R^2$	0.77	0.78	0.84	0.8
$R$	0.87	0.88	0.91	0.89

A mean error of zero and a standard error of estimate equal to 4.71 dB allow estimation of the basic transmission loss with satisfactory accuracy. In addition, the MCT model explains 80% of the path loss variability in the container terminal. It is indicated by the coefficient of determination, which equals 0.8. Furthermore, the correlation coefficient nearly equal to 0.9 indicates very good correlation between real path loss values and the results obtained from the new model.

For better verification of the MCT model, another set of measurement data was taken into account. This data set was obtained during an additional measurement campaign which was carried out after elaboration of the model and with the same rules as described in section II. This campaign was shorter (less than 40 000 measurement data were collected) and it was intended to evaluate the accuracy of the MCT model. The results (Table III) are similar to the previous case, which means that the model matches well to the experimental values of path loss obtained in the investigated environment.



TABLE III  
STATISTICAL EVALUATION OF THE MCT – ADDITIONAL SET OF MEASUREMENT DATA

Parameter	$L_{LOS}$	$L_{Cont}$	$L_{OffT}$	$L_{MCT}$
$N$	8 201	23 295	8 312	39 808
$ME$ [dB]	0.85	1.03	-0.26	0.72
$SEE$ [dB]	4.40	4.53	4.30	4.45
$R^2$	0.81	0.80	0.77	0.82
$R$	0.90	0.89	0.88	0.90

In Table IV the ME and SEE values for each sub-area and each frequency are compared. In the LOS and Containers Areas, in the case of 500 MHz and 4 GHz, the MCT model slightly overestimates path loss in relation to measured values. For 1 GHz and 2 GHz there is some underestimation of the basic transmission loss. For the Off-Terminal Area the underestimation takes place for 1 GHz and 4 GHz, and the overestimation for 500 MHz and 2 GHz, but for 500 MHz the

ME is the highest and equals almost 3 dB. For the LOS Area the SEE is from a range of 3.78 to 5.05 dB, for the Container Area it is between 4.64 and 5.01 dB and for the Off-Terminal Area the SEE range is from 3.72 to 5.23 dB, depending on the frequency. To summarize Table IV, there is no regularity in the distribution of errors in the various sub-areas and at different frequencies.

In the following section the example graphs of path loss for each sub-area and various parameters of the model are presented. The predicted values are depicted, as well as the measured values. In addition, the predicted values plus SEE (label: predicted+SEE) and minus SEE (label: predicted-SEE) are shown. In Fig. 12 the graphs for the LOS Area are shown. For each frequency measured values seem to correspond well to regression lines, except in the case of 4 GHz, where the measured values are below the regression line. In most cases, however, it is in  $\pm SEE$  interval.

TABLE IV  
THE EVALUATION FOR EACH SUB-AREA AND VARIOUS FREQUENCIES

	LOS Area			Containers Area			Off-Terminal Area		
	$ME$ [dB]	$SEE$ [dB]	$N$	$ME$ [dB]	$SEE$ [dB]	$N$	$ME$ [dB]	$SEE$ [dB]	$N$
0.5 GHz	-0.39	4.23	5 138	-1.10	4.64	23 005	-2.87	4.55	3 082
1 GHz	1.29	3.78	9 367	0.98	5.01	41 510	1.53	5.23	6 218
2 GHz	0.27	5.05	14 466	0.16	4.98	47 394	-0.05	3.98	8 763
4 GHz	-0.59	4.59	25 312	-0.13	4.67	84 330	0.07	3.72	11 132

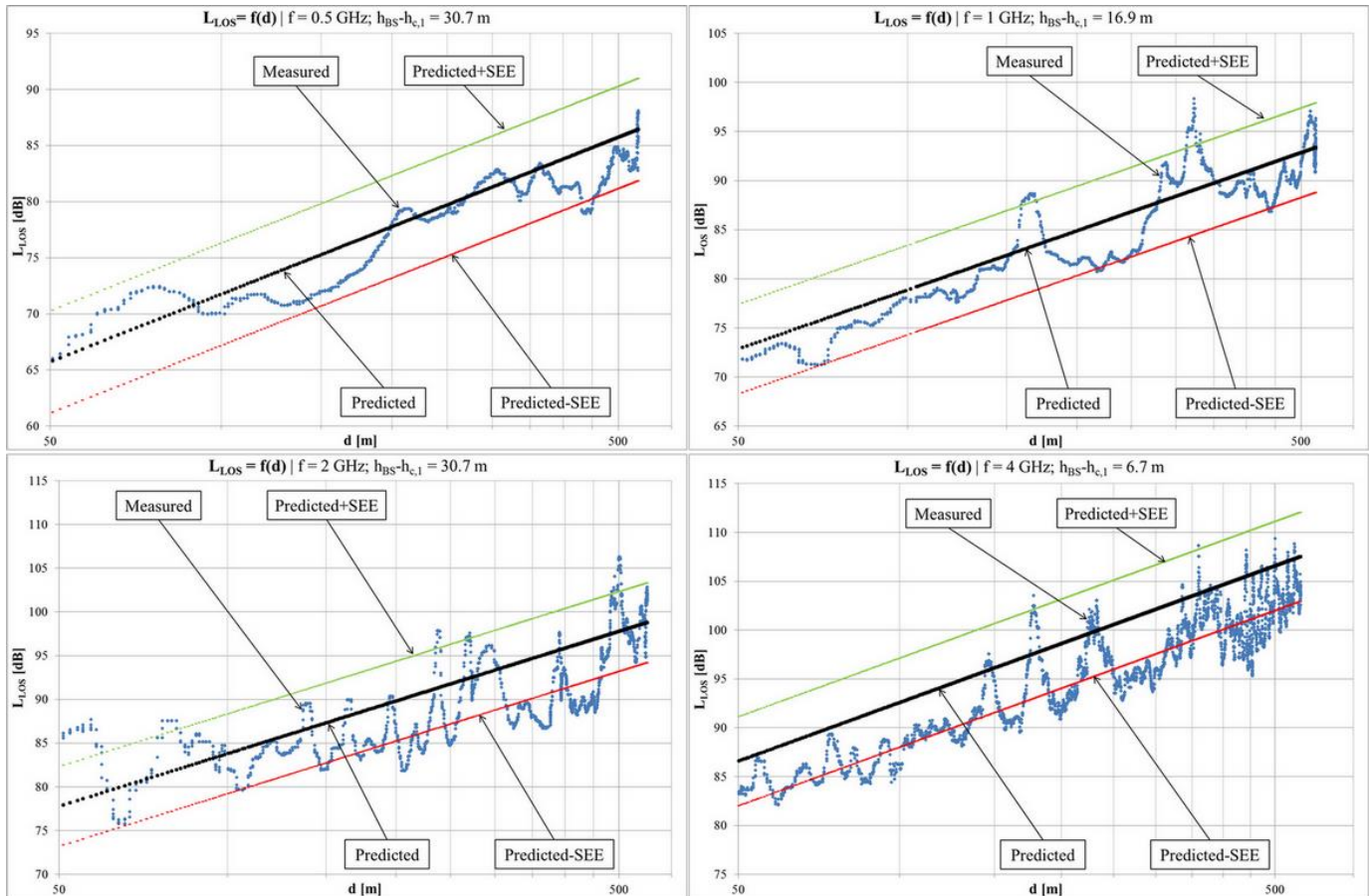


Fig. 12. Example path loss graphs for the LOS Area and for various frequencies.



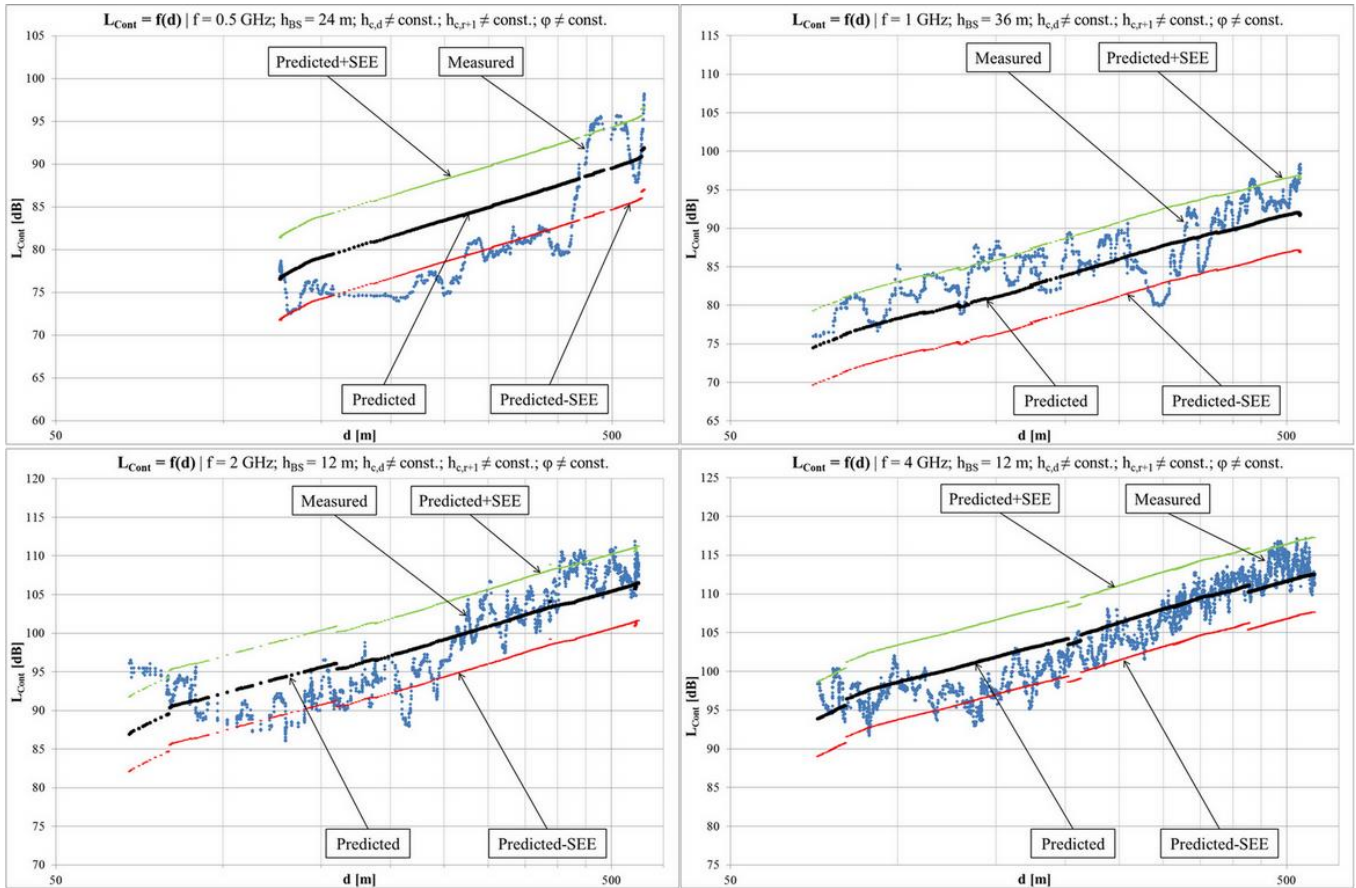


Fig. 13. Example path loss graphs for the Containers Area and for various frequencies.

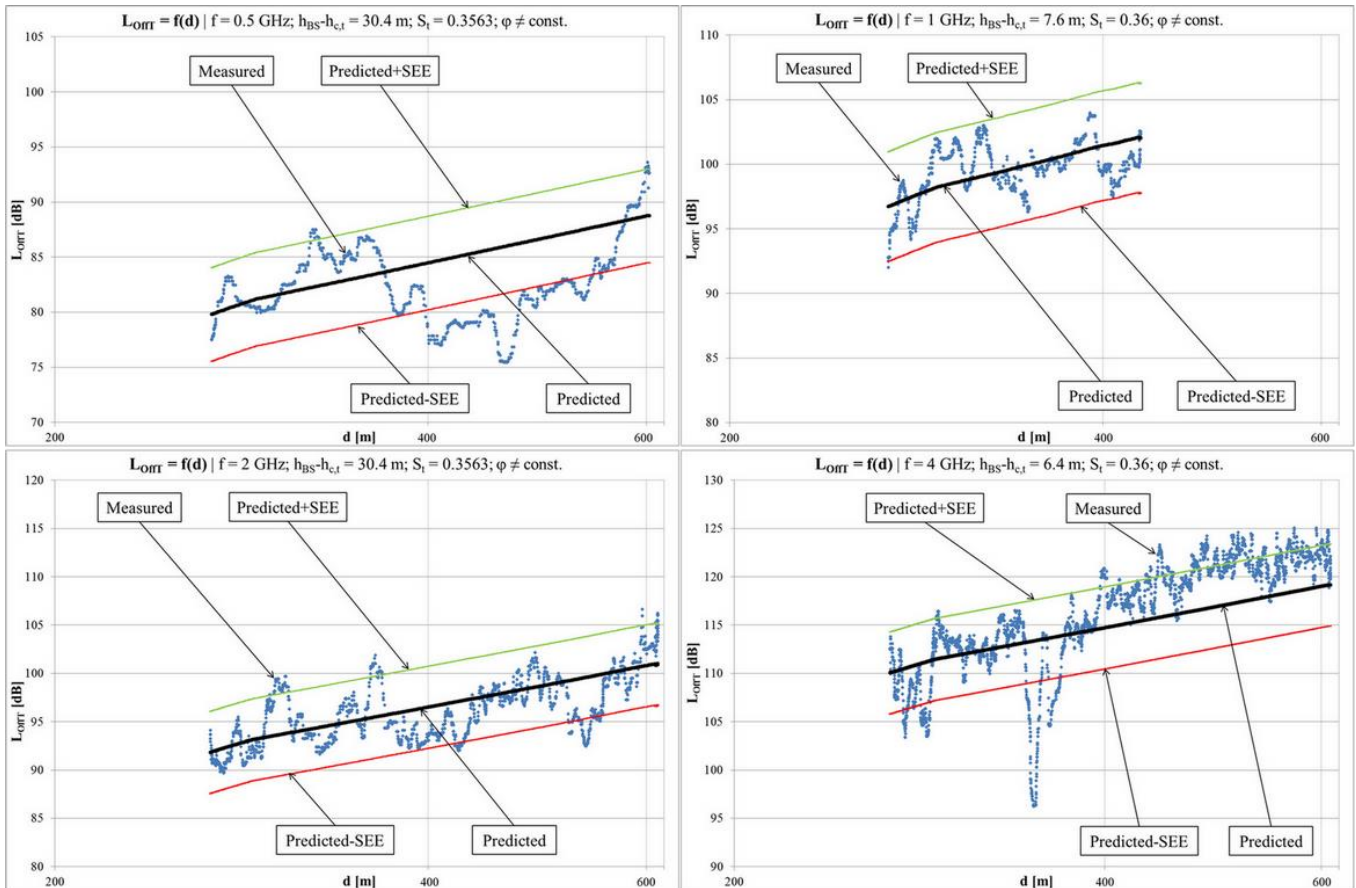


Fig. 14. Example path loss graphs for the Off-Terminal Area and for various frequencies.



In Fig. 13 the path loss comparison in the Containers Area at various frequencies is shown. It may be seen that for frequency 500 MHz, for distance  $d$  from a range of 150 m to 400 m, the empirical data are below the calculated values. This may result from a specific situation, namely when there are no container stacks on the particular path of radio wave. A similar situation (but on a smaller scale) is for 1 GHz, for a distance of about 350 m.

Graphs for the third area – the Off-Terminal Area – are depicted in Fig. 14. The specific situation, as described above, is for frequency 500 MHz for a distance from a range of 400 m to 500 m. Moreover, the decrease in the path loss at the distance of 350 m in the case of 4 GHz is very interesting (the graph in the bottom right-hand corner of Fig. 14.). It may be caused by the container truck being temporarily located behind the receiver. In such a situation, the signal reflected from the truck can be in phase with the diffracted signal from the base station, which may cause an increase in the received signal power and the decrease in the path loss.

The error distribution calculated as the differences between measured path loss ( $L_m$ ) and predicted path loss using the MCT model is shown in Fig. 15. This histogram of errors is for all sub-areas of the investigated environment.

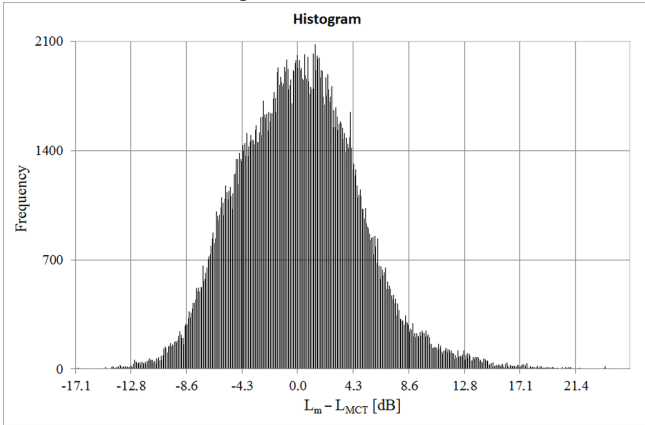


Fig. 15. Histogram of errors for measured and calculated values.

## VI. TUNING OF THE WALFISCH-IKEGAMI MODEL

Since the Walfisch-Ikegami model is commonly used to predict basic transmission loss, this model has been modified by tuning its coefficients. The COST231 Walfisch-Ikegami model was developed in the 1990s as a result of the COST 231 Project. The model makes it possible to improve path loss estimation by considering more data to describe the character of the urban environment, namely: heights of buildings, widths of roads, building separation, and road orientation with relation to the direct radio path. For a non-line-of-sight (NLOS) situation, the basic transmission loss is dependent on a free space loss  $L_0$ , a multiple screen diffraction loss  $L_{msd}$ , and a roof-top-to-street diffraction and scatter loss  $L_{rts}$  [2]. It is expressed as follows:

$$L_{WI[dB]} = \begin{cases} L_{0[dB]} + L_{rts[dB]} + L_{msd[dB]}, & \text{for } L_{rts} + L_{msd} > 0, \\ L_{0[dB]}, & \text{for } L_{rts} + L_{msd} \leq 0, \end{cases} \quad (12)$$

where:

$$L_{0[dB]} = 32.4 + 20 \log d_{[km]} + 20 \log f_{[MHz]}. \quad (13)$$

Considering that for the investigated environment the widths of roads ( $w$ ) equal 10 m, the average height of buildings is equivalent to the average height of container stacks ( $h_{c,t}$ ) throughout the terminal, and the street-orientation function ( $L_{ori}$ ) remains in its original form, the  $L_{rts}$  factor may be expressed as follows:

$$L_{rts[dB]} = -26.9 + 10 \log f_{[MHz]} + 20 \log (h_{c,t[m]} - h_{MS[m]}) + L_{ori[dB]}. \quad (14)$$

Assuming that for the investigated environment the building separation ( $b$ ) is equivalent to the separation of the main container fields, this parameter equals 29.9 m. Also, taking into account the fact that during measurements the base station antenna was installed above the average height of container stack ( $h_{BS} > h_{c,t}$ ), the  $L_{msd}$  factor may be expressed as follows:

$$L_{msd[dB]} = 40.7 - 18 \log \left[ 1 + (h_{BS[m]} - h_{c,t[m]}) \right] + 18 \log d_{[km]} + k_f \log f_{[MHz]}, \quad (15)$$

where:

$$k_f = -4 + 0.7 \left( \frac{f_{[MHz]}}{925} - 1 \right). \quad (16)$$

Other parameters in the above formulas have the same meaning as in the MCT model.

The proposition of the Walfisch-Ikegami model adjusted to the investigated environment is given by the following formula:

$$L'_{WI[dB]} = \begin{cases} L_{0[dB]} + L'_{rts[dB]} + L'_{msd[dB]}, & \text{for } L'_{rts} + L'_{msd} > 0, \\ L_{0[dB]}, & \text{for } L'_{rts} + L'_{msd} \leq 0, \end{cases} \quad (17)$$

where the parametric form of tuned roof-top-to-street diffraction and scatter loss:

$$L'_{rts[dB]} = -26.9 + p_1 \cdot 10 \log f_{[MHz]} + p_2 \cdot 20 \log (h_{c,t[m]} - h_{MS[m]}) + p_3 \cdot L_{ori[dB]}, \quad (18)$$

and the parametric form of tuned multiple screen diffraction loss:

$$L'_{msd[dB]} = 40.7 - p_4 \cdot 18 \log \left[ 1 + (h_{BS[m]} - h_{c,t[m]}) \right] + p_5 \cdot 18 \log d_{[km]} + p_6 \cdot k_f \log f_{[MHz]}. \quad (19)$$

The accuracy of path loss prediction in the container terminal environment can be improved by proper tuning of parameters:  $p_1, p_2, p_3, p_4, p_5, p_6$ . The tuning process was based on minimizing the standard error of estimate (SEE) expressed by (10), where  $L_{m,i}$  is the measured path loss value and  $L_{c,i}$  is the path loss value predicted by the tuned Walfisch-Ikegami model, expressed by (17). This was done on the basis of empirical data and using multivariate linear regression [23].

The obtained values of regression parameters are presented in Table V. The statistical significance (with a level of 5%) of each coefficient was proven using the  $t$ -test with Student's distribution.

TABLE V

REGRESSION PARAMETERS FOR THE TUNED WALFISCH-IKEGAMI MODEL

Parameter	$p_1$	$p_2$	$p_3$	$p_4$	$p_5$	$p_6$
Value	0.23	0.11	0.34	0.65	0.03	-0.21

After substitution of the parameters into (18) and (19), the following relations for each term were obtained:

$$L'_{rts[dB]} = -26.9 + 2.3 \log f_{[MHz]} + 2.2 \log (h_{c,t[m]} - h_{MS[m]}) + 0.34 L_{ori[dB]}, \quad (20)$$

$$L'_{msd[dB]} = 40.7 - 11.7 \log \left[ 1 + (h_{BS[m]} - h_{c,i[m]}) \right] + 0.54 \log d_{[km]} - 0.21 \cdot k_f \log f_{[MHz]}. \quad (21)$$

In addition, for comparative purposes, a simple model has been calculated. In this model the path loss ( $L_{simple}$ ) depends on the signal frequency ( $f$ ) and the path length ( $d$ ). It is described by following equation:

$$L_{simple[dB]} = 20 \log f_{[MHz]} + 21.8 \log d_{[m]} - 22.3. \quad (22)$$

Fig. 16 presents the example path loss graphs for original and tuned Walfisch-Ikegami model, for simple model and for the MCT model, for each measured frequencies, namely: 500 MHz, 1 GHz, 2 GHz and 4 GHz. In case of original and tuned Walfisch-Ikegami model, the improvement of path loss prediction is better for higher frequencies, especially for the case of 2 GHz and 4 GHz, where the original model significantly overestimates the measured values of the path loss. The simple model overestimates the measured path loss values, except the case of 4 GHz. The results for the MCT model and for the tuned Walfisch-Ikegami model are quite similar, especially for the case of 1 GHz, where regression lines are almost congruent.

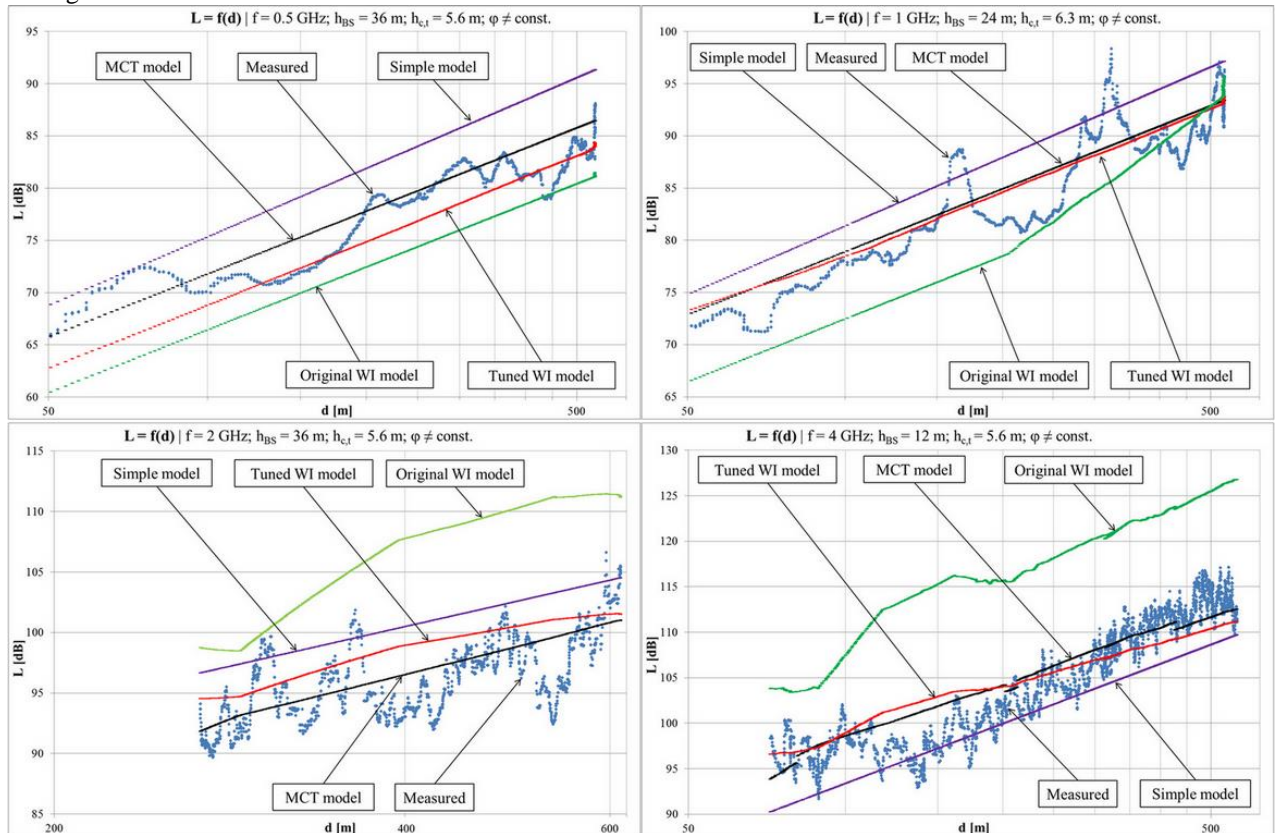


Fig. 16. Example path loss graphs for: original and tuned Walfisch-Ikegami model, simple model and the MCT model.

Table VI summarizes the values of mean error (ME), standard error of estimate (SEE), coefficient of determination ( $R^2$ ) and correlation coefficient ( $R$ ) for both the original and the tuned Walfisch-Ikegami model, for the simple model, and for the MCT model. These values were calculated for all measured data.

TABLE VI  
A COMPARISON OF ORIGINAL AND TUNED WALFISCH-IKEGAMI AND SIMPLE MODEL WITH MCT MODEL

Parameter	Original ( $L_{WI}$ )	Tuned ( $L'_{WI}$ )	Simple ( $L_{simple}$ )	MCT ( $L_{MCT}$ )
ME [dB]	-5.29	0.0	0.0	0.0
SEE [dB]	10.59	5.09	6.05	4.71
$R^2$	0.01	0.77	0.66	0.80
$R$	0.1	0.88	0.81	0.89

As can be seen, the original Walfisch-Ikegami provides the worst accuracy of path loss prediction. In case of the simple model the accuracy is better, but coefficient of determination is significantly lower than in case of tuned Walfisch-Ikegami and MCT model. It means that only 66% of path loss variability of propagation path loss is explained by the simple model. The tuned Walfisch-Ikegami model is significantly better than the original one, but worse than the new MCT model destined for the environment under investigation. However, values of SEE and  $R^2$  for tuned Walfisch-Ikegami and for MCT model are similar.

A comparison of three analysed models for particular sub-areas of container terminal is shown in Table VII. In each case the accuracy of the simple model is the worst in comparison with other models.

TABLE VII  
A COMPARISON OF TUNED WALFISCH-IKEGAMI AND SIMPLE MODEL WITH MCT MODEL FOR PARTICULAR SUB-AREAS OF CONTAINER TERMINAL

Subarea	LOS Area			Containers Area			Off-Terminal Area		
	Simple	Tuned WI	MCT	Simple	Tuned WI	MCT	Simple	Tuned WI	MCT
<i>ME</i> [dB]	-2.90	-0.79	0.00	0.80	0.25	0.00	0.47	-0.22	0.00
<i>SEE</i> [dB]	5.59	4.79	4.56	6.00	4.93	4.82	7.07	5.27	4.25
$R^2$	0.65	0.74	0.77	0.66	0.77	0.78	0.55	0.75	0.84
$R$	0.80	0.86	0.87	0.81	0.88	0.88	0.74	0.87	0.91

Considering the LOS Area and the Containers Area it can be seen, that accuracy of the MCT model is higher than the tuned Walfisch-Ikegami, but the difference is not significant. The situation is different for the Off-Terminal Area, where SEE is 1dB higher for the MCT model and the difference of coefficient of determination is also significant. It should be noted that from the point of view of the wireless network designer, the model accuracy for Off-Terminal Area is most important to ensure full radio coverage. Therefore the MCT model allows to estimate the path loss with higher accuracy in general.

## VII. CONCLUSION

It is worth noting that, as yet, there is no propagation model for designing mobile radio networks in the container terminal environment. Therefore, in practice other models are used. This yields large discrepancies in path loss estimation. Thus, there was a need to develop a novel empirical propagation model for mobile radio applications in such a complex environment as the container terminal described in this article. This new model (called MCT) takes into account all essential factors that occur in this environment and that affect basic transmission loss of radio wave.

The MCT model is the first model for the accurate estimation of path loss in the investigated environment. It was developed on the basis of almost 290 000 propagation path measurements in a real container terminal environment, collected in accordance with the appropriate requirements. The obtained standard error of estimate is 4.71 dB. What is more, the obtained value of the coefficient of determination is 0.8, and the correlation coefficient is 0.89, which additionally proves the accuracy and usefulness of the MCT model.

It should be noted that results obtained for the tuned Walfisch-Ikegami model are also satisfactory, but the comparison with the MCT model for the most crucial Off-Terminal Area indicates that the new model – dedicated to the container terminal environment – ensures more accurate path loss estimation. However, the difference between the proposed MCT model and the tuned COST231 model is small and possibly not significant with respect to measurement accuracy. The reasons for such an agreement between the two models remain to be further investigated. It would be of major interest to understand better the underlying physical phenomena leading to improved path loss modelling.

The MCT model may be used for frequencies from a range of 500 MHz to 4 GHz, propagation path length between 50 m and 620 m and base station antenna height between 12 m and 36 m. This model can be applied in container terminals of

different sizes, where the dimensions of main container fields are about 139.1 m long and about 19.9 m wide, and the main routes between these fields are about 10 m wide and the perpendicular routes are about 19.15 m wide.

The described model is a prelude to elaborating a more universal model for container terminal areas and for outdoor industrial environments in general. For this reason, comprehensive measurement research in different environments should be carried out. For obvious reasons this should be done in international cooperation.

## ACKNOWLEDGEMENTS

The authors would like to thank the reviewers for all their valuable comments and suggestions which greatly improved the quality of this article.

## REFERENCES

- [1] *Propagation Data and Prediction Methods for the Planning of Short-Range Outdoor Radiocommunication Systems and Radio Local Area Networks in the Frequency Range 300MHz to 100 GHz*, ITU-R P.1411-4, 2007.
- [2] D. J. Cichon and T. Kürner, "Propagation Prediction Models," in "Digital Mobile Radio Towards Future Generation Systems," COST 231 Final Report, 1999.
- [3] T. Kürner and M. Neuland, "Application of Bertoni's Work to Propagation Models used for the Planning of real 2G and 3G Cellular Networks," in *3rd European Conference on Antennas and Propagation*, Berlin, Germany, Vols. 1-6, 2009, pp. 1606-1610.
- [4] A. Hecker and T. Kürner, "Analysis of Propagation Models for UMTS Ultra High Sites in Urban Areas," in *IEEE 16th International Symposium on Personal, Indoor and Mobile Radio Communication – PIMRC 2005*, Berlin, Germany, Vol. 4, 2005, pp. 2337-2341.
- [5] N. C. Gonçalves and L. M. Correia, "A Propagation Model for Urban Microcellular System at the UHF Band," *IEEE Transactions on Vehicular Technologies*, vol. 49, no. 4, pp. 1294-1302, 2000.
- [6] *The Concept of Transmission Loss for Radio Links*, ITU-R P.341-5, 1999.
- [7] R. J. Katulski, J. Sadowski and J. Stefanski, "Propagation Path Modelling in Container Terminal Environment," in *Proc. of VTC 2008-Fall: IEEE 68th Vehicular Technology Conference*, Calgary, Canada, 2008, pp. 1-4.
- [8] S. J. Ambroziak, R. J. Katulski, J. Sadowski and J. Stefanski, "Propagation Path Loss Modelling in Container Terminal Environment," in *Vehicular Technologies: Increasing Connectivity*, InTech, 2011, pp. 415-432.
- [9] S. J. Ambroziak and R. J. Katulski, "On the Usefulness of Selected Radio Waves Propagation Models for Designing Mobile Wireless Systems in Container Terminal Environment," in *Proceedings of the XXX General Assembly and Scientific Symposium of URSI*, Istanbul, Turkey, 2011, pp. 1-4.
- [10] S. J. Ambroziak and R. J. Katulski, "Experimental Verification of Selected Propagation Models in Terms of Designing Mobile Radio Networks in Container Terminal Environment," in *12th URSI Commission F Triennial Open Symposium on Radio Wave Propagation and Remote Sensing*, Garmisch-Partenkirchen, Germany, 2011.
- [11] S. J. Ambroziak and R. J. Katulski, "Statistical Adjustment of Selected Propagation Models for Applications in Container Terminal," in *The 6th*



*European Conference on Antennas and Propagation – EuCAP 2012*, Prague, Czech Republic, 2012, pp. 3327 – 3331.

- [12] S. J. Ambroziak, “Empirical Adjustment of the Selected Propagation Models for Application in the Peculiar Environment of the Container Terminal,” in *The 2012 IEEE International Symposium on Antennas and Propagation and USNC-URSI National Radio Science Meeting*, Chicago, USA, 2012.
- [13] *Field-Strength Measurements Along a Route with Geographical Coordinate Registration*, ITU-R SM.1708, 2005.
- [14] W. C. Y. Lee, *Mobile Communications Design Fundamentals*, 2nd ed., Wiley, 1993.
- [15] W. C. Y. Lee, “Estimate of Local Average Power of a Mobile Radio Signal,” *IEEE Transactions on Vehicular Technologies*, vol. 34, no. 1, pp. 22-27, 1985.
- [16] C.A. Levis, J.T. Johnson, F.L. Teixeira, *Radiowave Propagation. Physics and Application*, Wiley, 2010.
- [17] *Attenuation by Atmospheric Gases*, ITU-R P.676-9, 2012.
- [18] *Propagation Data and Prediction Methods Required for the Design of Terrestrial Line-of-Sight System*, ITU-R P.530-14, 2012.
- [19] F. Ikegami, S. Yoshida, T. Takeuchi, M. Umehira, “Propagation Factors Controlling Mean Field Strength on Urban Streets,” *IEEE Transactions on Antennas and Propagation*, vol. 32, no. 8, pp. 822-829, 1984.
- [20] T. Kürner, D. J. Cichon, W. Wiesbeck, “The Influence of Land Usage on UHF Wave Propagation in the Receiver Near Range,” *IEEE Transactions on Vehicular Technologies*, vol. 46, no. 3, pp. 739-747, 1997.
- [21] R. J. Katulski, A. Kiedrowski, “Calculation of the propagation loss in urban radio-access systems,” *IEEE Antennas and Propagation Magazine*, vol. 50, no. 6, pp. 65-70, 2008.
- [22] R. J. Katulski, “Method of Statistical Evaluation of Experimental Results,” in *Radio Wave Propagation in Wireless Telecommunication* (in Polish), WKL, Warsaw, 2000.
- [23] H. Cramer, *Mathematical Methods of Statistics*, Princeton University Press, 1999.



**Slawomir J. Ambroziak** was born in Koszalin, Poland, in 1982. He received the M.Sc. degree in radio communication in 2008 and the Ph.D. degree in radio communication in 2013 from the Gdansk University of Technology (GUT), Gdansk, Poland.

Since 2008 he is with the Radio Communication Department of the GUT, from 2008 to 2013 as Research Assistant and since 2013 as Assistant Professor. Before 2008 he gained experience in radio communication equipment designing and installing, during his work in industry, firstly as a designer and

later as a design and assembly team manager. He is an author or co-author of more than 70 publication including book chapters, articles, reports and papers presented during international and domestic conferences. He participated in several projects related to special application of wireless techniques. His research interests include wireless communication and radio wave propagation.

Dr. Ambroziak was a recipient of the Young Scientists Award of URSI in 2011, the Eighth International Conference on Wireless and Mobile Communications Best Paper Award in 2012, and many domestic awards. He is a member of the EurAAP Working Group on Propagation and a participant at COST-IC1004 Action.



**Ryszard J. Katulski** (M'90) was born in Gniezno, Poland, in 1948. He received the M.Sc. degree in radio communications from the Gdansk University of Technology (GUT), Gdansk, Poland, in 1975, the Ph.D. degree from the Wroclaw University of Technology, Wroclaw, Poland, in 1984 and the D.Sc. degree from the Military University of Technology, Warsaw, Poland, in 1999.

Since 1968 he is with the Radio Communication Department of the GUT, from 1976 to 1984 as Senior Assistant, from 1985 to 2000 as Assistant Professor, from 2000 to 2005 as Associate Professor and from 2005 as Professor of the GUT. From 2005 to 2008 he was the vice-Rector for Researches and Applications of the GUT and from 2002 to 2005 he was the vice-Dean of the Electronics, Telecommunications and Informatics Faculty of the GUT. His research interests include wireless communications and electromagnetic compatibility, especially antennas, propagation and EMC analysis. He is the author or co-author more than 350 technical papers published in peer-reviewed journals and presented at domestic

and international conferences, and the author of book about radio wave propagations (in Polish) and the co-author of 13 book chapters. He conducted several projects related to special applications of wireless techniques. In May 1994 he visited Tokyo University of Agriculture and Technology, Japan, as EMC measurements visited researcher.

Prof. Katulski is a member of the IEICE, Japan and a member of the EurAAP Working Group on Propagation.

